



**Environmental  
Science**  
Water Research & Technology

**Seasonal Treatment and Economic Evaluation of an Algal  
Wastewater System for Energy and Nutrient Recovery**

Journal:	<i>Environmental Science: Water Research &amp; Technology</i>
Manuscript ID	EW-ART-03-2019-000242.R1
Article Type:	Paper
Date Submitted by the Author:	01-Jun-2019
Complete List of Authors:	Li, Yalin; Colorado School of Mines, Civil and Environmental Engineering; University of Illinois at Urbana-Champaign, Institute for Sustainability, Energy, and Environment Slouka, Sydney; Colorado School of Mines, Civil and Environmental Engineering Henkanatte-Gedera, Shanka; New Mexico State University, Civil and Environmental Engineering; Pacific Advanced Civil Engineering Inc. Nirmalakhandan, Nagamany; New Mexico State University, Civil and Environmental Engineering Department Strathmann, Timothy; Colorado School of Mines, Civil and Environmental Engineering; National Renewable Energy Laboratory, National Bioenergy Center

SCHOLARONE™  
Manuscripts

## **Water Impact Significance**

Wastewater is attracting growing attention as a potential source for valuable products. This study describes an integrated system where microalgae is used to treat primary clarified municipal wastewater in different seasons, and the harvested algal biomass is converted to biofuels and fertilizers via hydrothermal processing. Economic analysis of conversion processes is performed and shows promising results of such systems.

# 1           **Seasonal Treatment and Economic Evaluation of an Algal** 2           **Wastewater System for Energy and Nutrient Recovery**

3                   Yalin Li<sup>a,b,†</sup>, Sydney A. Slouka<sup>a,b</sup>, Shanka M. Henkanatte-Gedera<sup>b,c,§</sup>,

4                   Nagamany Nirmalakhandan<sup>b,c</sup>, Timothy J. Strathmann<sup>\*,a,b,d</sup>

5           <sup>a</sup>Department of Civil and Environmental Engineering, Colorado School of Mines, Golden, CO  
6           80401, USA

7           <sup>b</sup>Engineering Research Center for Re-inventing the Nation's Urban Water Infrastructure  
8           (ReNUWIt), USA

9           <sup>c</sup>Civil Engineering Department, New Mexico State University, Las Cruces, NM 88003, USA

10          <sup>d</sup>National Bioenergy Center, National Renewable Energy Laboratory, Golden, CO 80401, USA

11          <sup>†</sup>Present address: Institute for Sustainability, Energy, and Environment, University of Illinois at  
12          Urbana-Champaign, Urbana, IL 61801, USA

13          <sup>§</sup>Present address: Pacific Advanced Civil Engineering Inc., Fountain Valley, CA 92708, USA

14          \*Corresponding author: T. Strathmann, E-mail: strthmnn@mines.edu, Phone: +1 (303) 384-2226

## 15          **Abstract**

16          Algal systems have been proposed for treating wastewater while simultaneously recovering energy  
17          and nutrients. In this study, an integrated system with algal treatment of municipal wastewater  
18          followed by hydrothermal liquefaction (HTL) conversion and upgrading steps was evaluated.  
19          Pilot-scale treatment of primary clarified municipal wastewater effluent was evaluated in different  
20          seasons (cold, warm, and a transitional period in between) with different strains of algae selected  
21          for each season, and the warm season strain successfully met all local discharge regulations. The  
22          collected wastewater algae biomass was subjected to HTL at 300 and 350°C and both energy and  
23          nutrient recoveries were much improved at the higher temperature. The transitional batch was  
24          found to have the highest biocrude oil yields, and its co-products had the highest nutrient (nitrogen  
25          and phosphorus) contents. Economic analysis of conversion processes informed by the observed

26 HTL product yields was conducted. While this revealed that targeting biofuel products alone was  
27 not profitable, adding nutrient co-products (e.g., ammonium sulfate fertilizer), adjusting algae  
28 harvesting time, and incorporating component-specific conversion processes could substantially  
29 improve system economics. Overall, this study highlights connections between treatment and  
30 conversion processes, and demonstrates how these connections can be leveraged for more efficient  
31 resource recovery without compromising treatment operations.

## 32 **1 Introduction**

33 Growing demands for energy, food, and water are placing new stresses on society, and  
34 municipal wastewater is attracting increasing interest as a potential resource that can be exploited  
35 to help meet these needs.<sup>1-3</sup> However, conventional wastewater treatment plants use energy-  
36 intensive treatment strategies (e.g., aeration-based heterotrophic biological treatment) that focus  
37 on meeting discharge requirements through simple removal or down-cycling.<sup>4</sup> For example,  
38 secondary treatment via activated sludge processes converts nearly 50% of the dissolved organic  
39 carbon to CO<sub>2</sub>, nitrification-denitrification operations aim to remove nitrogenous constituents as  
40 N<sub>2</sub> gas, and chemical precipitation sequester phosphorus as poorly bioavailable solids—all terminal  
41 products with limited market value.<sup>4,5</sup>

42 As an alternative to dissimilative bacterial treatment processes, algae can purify wastewater by  
43 metabolically assimilating both organic carbon and nutrients present in wastewater, and the  
44 resulting biomass that accumulates can be harvested, concentrated, and processed with biorefinery  
45 technologies to generate valuable products, including fuels and fertilizers.<sup>6</sup> Revenues from these  
46 product streams can potentially reduce the cost of wastewater treatment or even flip the economic  
47 balance. Toward this end, several recent studies have explored the economic feasibility of large-  
48 scale biorefineries featuring a central hydrothermal liquefaction (HTL) conversion process

49 followed by a suite of upgrading steps for algal fuels.<sup>7-9</sup> It is concluded that the cost for algae  
50 production accounts for >50% of the overall cost,<sup>7-9</sup> which is expected to be lower for wastewater-  
51 algae given the co-location with wastewater treatment plant and the reduction in carbon and  
52 nutrient substrates.<sup>10</sup> However, existing studies that investigated the economic feasibility of  
53 wastewater-derived algal biofuels predominantly used product yields reported for freshwater-  
54 cultivated algae or other biomass.<sup>11-13</sup> As conversion yields and characteristics of the HTL  
55 products – which can vary significantly for different algal biomass<sup>14</sup> – have great influence on the  
56 overall economic performance of the system,<sup>7-9</sup> and wastewater algae are reported to have different  
57 properties from algae cultivated in other media (e.g., freshwater, saltwater).<sup>15,16</sup> This will result in  
58 over-estimation of total biofuel yields and more optimistic economic performance. Further, as  
59 nutrient co-products (e.g., fertilizers) are needed for algal fuels to be economically  
60 competitive,<sup>7,8,17</sup> it is important to examine potential revenues from these co-products, which have  
61 been largely overlooked in previous studies. Finally, as wastewater algae produced from different  
62 treatment operations (e.g., cold versus warm seasons, different treatment times) can have  
63 distinguishable properties and lead to variations in valuable product yields and system  
64 economics,<sup>4,18</sup> it is critical to study algae treatment and conversion systems as a whole to  
65 understand and leverage the dynamic interactions between treatment and conversion processes for  
66 more robust system performance.

67 In this study, a pilot-scale algal system was experimentally evaluated for treatment of primary  
68 municipal wastewater. The treatment experiments were conducted in different seasons (cold,  
69 warm, and a transitional period in between) with algal strains adapted for each season. The  
70 harvested algal biomass was then subjected to HTL conversion. Experimental yields and  
71 characteristics of the HTL products were used to inform model predictions of energy and nutrient

72 recoveries via aqueous conversion processes that were recently demonstrated with wastewater  
73 algal feedstocks.<sup>9</sup> Finally, economic analysis of conversion processes was conducted with  
74 sensitivity and uncertainty analyses and evaluated under different scenarios to assess economic  
75 feasibility of the system and identify future research priorities.

## 76 **2 Materials and Methods**

### 77 **2.1 Pilot-scale algal wastewater treatment**

78 Treatment experiments were conducted with primary effluent from the Jacob A. Hands  
79 Wastewater Treatment Plant (Las Cruces, NM, USA). Local discharge standards at the treatment  
80 facility are 30 mg O<sub>2</sub>·L<sup>-1</sup>, 10 mg N·L<sup>-1</sup>, and 1 mg·L<sup>-1</sup>, for 5-day biochemical oxygen demand  
81 (BOD<sub>5</sub>), NH<sub>4</sub><sup>+</sup>-N, and PO<sub>4</sub><sup>3-</sup>, respectively. A mixotrophic algal species, *Galdieria sulphuraria*, was  
82 selected due to its versatile metabolism that could leverage both CO<sub>2</sub> and organic substrates as the  
83 carbon source,<sup>19</sup> thus realizing the removal of organic carbon and nutrients in a single stage.<sup>20</sup> To  
84 evaluate treatment efficiency and energy and nutrient recovery potentials of the harvested algae  
85 during different seasons, two strains of *G. sulphuraria* – Soos and CCMEE 5587.1 – were selected  
86 for cold (mid-December to March) and warm (May to September) seasons, respectively. Soos was  
87 originally isolated from a diatomite shield site in the National Nature Reserve Soos, Czech  
88 Republic<sup>21</sup> and CCMEE 5587.1 was identified by the Culture Collection of Microorganisms from  
89 Extreme Environments at the University of Oregon.<sup>5</sup> Soos was chosen for its ability to maintain  
90 comparable properties (e.g., ultrastructure, fatty acid composition, thermostability of enzymes) at  
91 much lower temperatures than other *G. sulphuraria* strains with similar substrates;<sup>21</sup> and CCMEE  
92 5587.1 was selected as previous studies had reported promising organic carbon and nutrient  
93 removal rates at pilot scale.<sup>5</sup>

94 *G. sulphuraria* was grown in three 700 L parallel pilot-scale photobioreactors in a raceway  
95 configuration. The photobioreactors were enclosed in translucent polyethylene growth bags to  
96 minimize evaporation and keep culture temperature at much higher levels than ambient air. The  
97 photobioreactors were operated with natural photoperiod and light intensity with headspace filled  
98 with 2% CO<sub>2</sub>-enriched air. Each treatment experiment was initiated with 400 L of wastewater and  
99 300 L of cultures (preadapted with wastewater for 5 days prior to experiments). Four batches of *G.*  
100 *sulphuraria* biomass were harvested from different treatment experiments and subjected to HTL  
101 reactions: one composed of cold strain Soos generated under batch operating conditions (referred  
102 to as Cold-B, culture temperature during treatment at 13–37°C, a summary of treatment conditions  
103 is provided in Table S1 in the Electronic supplementary information, ESI); one composed of warm  
104 strain CCMEE 5587.1 generated under batch operating conditions (referred to as Warm-B, culture  
105 temperature during treatment at 31–46°C); one composed of a polyculture generated during the  
106 transitional period from CCMEE 5587.1 to Soos under batch operating conditions (referred to as  
107 Trans-B, culture temperature during treatment at 10–27°C, made from 1:1 volumetric ratio mixture  
108 of Cold-B and Warm-B seed culture of similar biomass densities); and the last sample consisted  
109 CCMEE 5587.1 collected during warm season under fed-batch operating conditions (referred to  
110 as Warm-FB, culture temperature during treatment at 27–42°C). Under batch operation, all pilot  
111 treatment tests were terminated after 10 days; under fed-batch operation, upon meeting all  
112 discharge standards, 400 L of the algal-treated wastewater in each reactor was discharged (and  
113 biomass solids collected) and the reactors were replenished with fresh primary effluent to start a  
114 new treatment cycle. Depending on the influent contaminant levels, each fed-batch cycle took 2–  
115 3 days to reach all discharge standards, and the fed-batch test lasted 5 cycles over a period of 20  
116 days. BOD<sub>5</sub>, NH<sub>4</sub><sup>+</sup>-N, and PO<sub>4</sub><sup>3-</sup> were monitored according to a previous study.<sup>5</sup> BOD<sub>5</sub> was

117 measured in duplicate, and  $\text{NH}_4^+\text{-N}$  and  $\text{PO}_4^{3-}$  were measured in triplicate. For purposes of  
118 experimental expediency, all harvested biomass samples were freeze-dried, ground to powder, and  
119 preserved at  $4^\circ\text{C}$  for subsequent analyses or use in HTL experiments.

## 120 **2.2 Characterization of wastewater algal biomass**

121 Biochemical and elemental compositions of the harvested biomass were analyzed following  
122 procedures described previously.<sup>14</sup> Briefly, moisture contents were determined by mass loss at  
123  $105^\circ\text{C}$ . Ash contents were determined by remaining mass after ignition at  $550^\circ\text{C}$ . Elemental  
124 carbon, hydrogen, and nitrogen contents were analyzed using an Exeter CE-440 Elemental  
125 Analyzer (University of Illinois Microanalysis Laboratory, Urbana, IL). Phosphorus contents were  
126 measured by ICP-AES (PerkinElmer 5300DV) following acid digestion according to EPA method  
127 3052.<sup>22</sup> Volatile oxygen contents were estimated by difference ( $100 - \text{C}\% - \text{H}\% - \text{N}\% - \text{P}\% - \text{Ash}\%$ ,  
128 all on dry weight basis,  $\text{dw}\%$ ). Gross lipid contents were estimated by solvent extraction with a  
129 2:1 (v/v) chloroform:methanol mixture. Protein contents were calculated from nitrogen contents  
130 using a nitrogen-to-protein conversion factor of 6.25;<sup>23</sup> carbohydrate contents were measured by a  
131 colorimetric assay using 3-methyl-2-benzothiazolinone hydrazone. All characterizations were  
132 conducted in duplicate (moisture and ash contents were measured in triplicate).

## 133 **2.3 HTL experiments and product analyses**

134 HTL experiments were conducted in tube reactors with dimension of  $3'' \times 1/2''$  (L  $\times$  OD, wall  
135 thickness was  $0.049''$ ) and volume of 6.24 mL. Algal slurries of 20  $\text{dw}\%$  were prepared with  
136 freeze-dried algae and deionized (DI) water, and 4.2 g and 3.0 g of slurries were added to reactors  
137 for experiments conducted at 300 and  $350^\circ\text{C}$ , respectively (to account for water density differences  
138 at the two conditions<sup>24</sup>). Reactors were placed into a preheated kiln (Paragon Sentry 2.0) at the

139 designated temperature for 60 min. Tubes were then placed in room-temperature water to quench  
140 further reactions. Detailed protocols used for separation and recovery of HTL products are  
141 described elsewhere.<sup>14</sup> Briefly, the reactor was opened to vent gaseous products, and the gas yield  
142 was determined by weighing the reactor before and after venting. Contents of the reactor were then  
143 poured into a beaker, and the reactor was rinsed sequentially with dichloromethane (DCM) and DI  
144 water to recover the biocrude and aqueous residuals, respectively. The resulting mixture was then  
145 filtered (0.45  $\mu\text{m}$  PTFE) to separate the solid biochar product, the yield of which was determined  
146 by the mass difference of dried filters before and after filtration. Biocrude oil (in DCM) and  
147 aqueous products in the filtrate were then separated by a separatory funnel and dried to determine  
148 the biocrude and aqueous total dissolved solids (TDS) yields.

149 Carbon, hydrogen, and nitrogen contents of biocrudes and biochars were determined in the  
150 same manner as biomass, and volatile oxygen contents of biocrudes were estimated by difference  
151 ( $100 - \text{C}\% - \text{H}\% - \text{N}\% - \text{Ash}\%$ , all on weight basis, wt%). Total organic carbon (TOC) of the  
152 aqueous products was analyzed by a Shimadzu TOC-LCSH analyzer, and total nitrogen (TN) by  
153 a Shimadzu TNM-L analyzer.  $\text{NO}_2^-$ ,  $\text{NO}_3^-$ , and  $\text{PO}_4^{3-}$  contents of aqueous products were analyzed  
154 by a Thermo Fisher Scientific Dionex 900 system ( $\text{NO}_2^-$  and  $\text{NO}_3^-$  contents were below detection  
155 limits for all batches).  $\text{NH}_4^+$ -N was analyzed using a phenate colorimetric method.<sup>25</sup>

## 156 **2.4 Energy calculations**

157 Higher heating values (HHVs) of algal biomass samples and the HTL biocrude products were  
158 calculated from elemental composition using Dulong's equation.<sup>14</sup> For 1 kg of dry algae, feedstock  
159 energy was represented by HHV of the algae; energy recovered in biocrude was calculated as the  
160 product of biocrude yield (dw%) and biocrude HHV; energy recovery of biocrude was defined as  
161 the percentage of feedstock energy recovered in biocrude (dw%); input heating requirements were

162 defined as the energy required to heat 5 kg of algae slurries (containing 1 kg of dry biomass and 4  
163 kg of water) from 25°C to the designated temperatures (300 or 350°C), assuming a heat recovery  
164 efficiency of 0.5, and combustion energy efficiency of 0.7.<sup>26</sup> Energy content of the biochar  
165 products were not considered due to their low organic contents.

## 166 **2.5 Economic analysis of conversion processes**

167 Experimental yields and characteristics of HTL products obtained from this study were used  
168 as inputs for a techno-economic analysis model<sup>7</sup> developed for production of algal biofuels  
169 (energy-related processes in **Figure 1**). Unlike previous model, which assumed a zero net present  
170 value to calculate the minimum selling price of biofuels, price of biofuel was set at \$2.79 gal<sup>-1</sup> as  
171 commercial gasoline, which is the average price for gasoline for the past 10 years (2010–2019)  
172 reported by U.S. Energy Information Administration (EIA).<sup>27</sup> This adjustment would allow  
173 comparison of revenues between biofuels and potential nutrient co-products (revenues from the  
174 latter not included in the original model<sup>7</sup>, but were calculated separately in this study) under  
175 different scenarios. Only conversion of algal biomass was included (i.e., neither costs nor credits  
176 associated with the treatment processes were considered) due to lack of well-established large-  
177 scale studies on economics of algal wastewater treatment processes. Production of wastewater  
178 algae was set to 25.6 U.S. ton per day on dry weight basis (TPD) based on a recent study, which  
179 equaled the amount of algae biomass generation expected from a 15-million-gallon-per-day (MGD)  
180 wastewater treatment plant.<sup>28</sup> Harvested wastewater algae was sent to a nearby algal conversion  
181 plant (i.e., no transportation cost was considered) with a processing rate of 576 TPD.<sup>7</sup> It should be  
182 noted that because of the economy of scale, it is unlikely for a conversion plant to be operated at  
183 a size that can be supported by a single algal wastewater treatment plant,<sup>7,28</sup> therefore size of the  
184 conversion plant was set based on recent studies on algal biofuel production.<sup>7,29</sup> The conversion

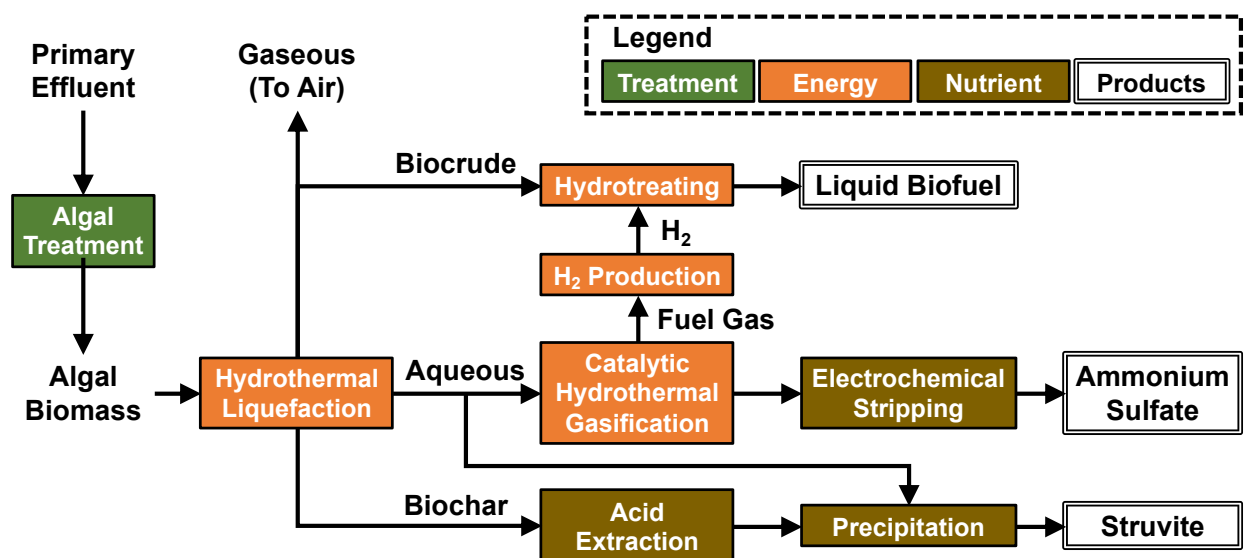
185 plant was assumed to use algal biomass feeds from other sources (e.g., algal farms) to compensate  
186 the differences, which were assumed to have a biochemical composition of 32.1% lipids, 14.3%  
187 proteins, 53.6% carbohydrates (on ash-free dry weight basis, averaged composition of *Chlorella*  
188 species modeled in the previous study on algal biofuel).<sup>7</sup> All costs were calculated using  
189 composition of the mixed algae stream (weighted average of *Chlorella* and wastewater algae from  
190 this study), but revenues were calculated from biofuel yields based on experimental results for  
191 wastewater algae reported in this study. In the conversion plant, the algal biomass was first  
192 processed via HTL to generate biocrude, aqueous, gaseous, and biochar products. Then the HTL  
193 biocrude was further upgraded to liquid hydrocarbon fuels in the gasoline and diesel range via  
194 established refinery hydrotreating and hydrocracking operations (**Figure 1**). Residual organic  
195 carbon in the aqueous product phase were converted to fuel gas via catalytic hydrothermal  
196 gasification (CHG). The generated liquid biofuels were sold for revenues while fuel gases  
197 generated in hydrotreating and CHG (rich in H<sub>2</sub> and CH<sub>4</sub>) were used internally (e.g., for production  
198 of H<sub>2</sub> for hydrotreating).<sup>30,31</sup>

199 The total cost included capital, operating, and financial costs. All costs were first calculated  
200 for the entire conversion plant at the size of 576 TPD, then prorated to the 25.6 TPD of the assumed  
201 wastewater algae inputs. Capital costs included costs of equipment (including installation),  
202 warehouse buildings, site development, additional piping, and other indirect costs (e.g., project  
203 contingency, working capital). Total capital costs (excluding working capital, which would be paid  
204 back at the end of operation) were calculated and annualized to each year as capital depreciation;  
205 operating costs included labor, maintenance, insurances and taxes, catalysts, utilities (water,  
206 natural gas, electricity); financial costs included income tax (35%) and loan payments based on a  
207 40% equity (i.e., 40% of the capital investment was provided by shareholders and 60% from loan),

208 8% loan interest rate for 10 years, and a 10% internal rate of return (IRR, determines the present  
209 value of future cashflows). No cost or credit were considered for the algal biomass, which would  
210 be generated from the wastewater treatment process. All prices were converted to 2014 U.S. dollars  
211 using GDP chain-type price index reported by U.S. EIA.<sup>27</sup> Detailed breakdown of the costs and  
212 calculates are provided in the ESI. To evaluate impacts from key assumptions, sensitivity and  
213 uncertain analyses were conducted for biofuel price, plant scale, total capital cost, total operating  
214 cost, project equity, and IRR. The range for biofuel price was determined based on the minimum  
215 (\$2.00 gal<sup>-1</sup>) and maximum (\$3.59 gal<sup>-1</sup>) gasoline prices reported by U.S. EIA between 2010–  
216 2019;<sup>27</sup> project equity was evaluated for a minimum of 0% (all capital investment from loan) and  
217 a maximum of 100% (all capital investment from shareholders); IRR was evaluated for a minimum  
218 of 0% and a maximum of 20%; plant scale, total capital cost, and total operating cost were  
219 evaluated for a minimum of 90% and a maximum of 110% of the baseline values.

220 Based on a previous study,<sup>9</sup> ammonium in CHG aqueous product could be recovered as  
221 ammonium sulfate fertilizer following electrochemical stripping, and phosphorus in HTL biochar  
222 product could be extracted and combined with a portion of HTL aqueous product for the  
223 production of magnesium ammonium phosphate ( $\text{MgNH}_4\text{PO}_4 \cdot 6\text{H}_2\text{O}$ , MAP or struvite) fertilizer  
224 (nutrient-related processes in **Figure 1**). Due to the lack of well-established large-scale studies on  
225 electrochemical stripping and struvite production by similar approaches, capital and operating  
226 costs for these two processes were not available, but revenues from the nutrient co-products were  
227 calculated based on properties of HTL products generated in this study and HTL product upgrading  
228 efficiencies reported previously.<sup>9</sup> As biochemical composition of algae changes during the  
229 treatment, additional analyses were conducted to understand the implication of different harvesting  
230 time. Biochemical composition of algae at their peak storage levels (i.e., highest levels of lipid and

231 carbohydrate contents) were calculated based on changes of lipid:protein and carbohydrate:protein  
 232 ratios during their growth to represent the maximum lipid and carbohydrate contents (ash contents  
 233 on dry weight basis assumed to be the same).<sup>18</sup>



234  
 235 **Figure 1.** Scheme of processes investigated in this study, energy-related processes were included  
 236 in the techno-economic analysis model,<sup>7</sup> costs for nutrient-related processes were not included,  
 237 but revenues from nutrient co-products are discussed in Section 3.5.

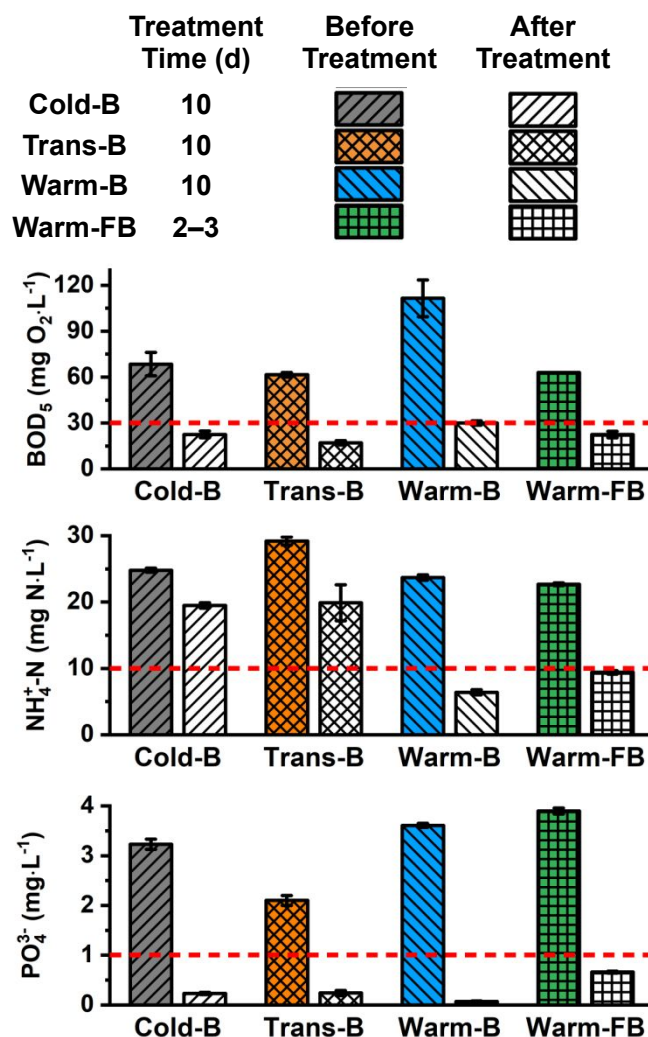
### 238 3 Results and Discussion

#### 239 3.1 Characteristics and treatment of wastewater

240 Characteristics of the primary wastewater effluent used as influent to the photobioreactors were  
 241 generally consistent throughout the year for  $\text{NH}_4^+\text{-N}$  (22.7–29.2  $\text{mg N}\cdot\text{L}^{-1}$ ) and  $\text{PO}_4^{3-}$  (2.1–3.9  
 242  $\text{mg}\cdot\text{L}^{-1}$ ), but fluctuations were observed in  $\text{BOD}_5$ , which nearly doubled for the Warm-B test  
 243 compared to others (111.5  $\text{mg O}_2\cdot\text{L}^{-1}$  versus 61.5–68.5  $\text{mg O}_2\cdot\text{L}^{-1}$ , **Figure 2** and Table S1 in the  
 244 ESI). However, the elevated  $\text{BOD}_5$  level didn't compromise the quality of algal-treated effluent,  
 245 and though the treatment experiment lasted for 10 days, all discharge standards were met within 4  
 246 days. This finding corresponded well with past reports showing that the warm season strain of *G.*  
 247 *sulphuraria* was capable of reducing all contaminants to their respective discharge levels within

248 3–4 days.<sup>5</sup> In sharp contrast to the Warm-B experiments, the Cold-B and Trans-B tests containing  
249 the cold strain Soos were not as effective in  $\text{NH}_4^+\text{-N}$  removal. While both  $\text{BOD}_5$  ( $30 \text{ mg O}_2\cdot\text{L}^{-1}$ )  
250 and  $\text{PO}_4^{3-}$  ( $1 \text{ mg}\cdot\text{L}^{-1}$ ) discharge standards were met,  $\text{NH}_4^+\text{-N}$  levels exceeded the discharge limit  
251 of  $10 \text{ mg N}\cdot\text{L}^{-1}$  for these two experiments ( $19.5$  and  $19.9 \text{ mg N}\cdot\text{L}^{-1}$  for Cold-B and Trans-B,  
252 respectively). Therefore, though all three batch runs resulted in comparable performance for  $\text{BOD}_5$   
253 and  $\text{PO}_4^{3-}$ , removal of  $\text{NH}_4^+\text{-N}$  followed the order of Warm-B >> Trans-B > Cold B. As the Trans-B  
254 test was seeded with a mixture of warm and cold strains of *G. sulphuraria*, it can be concluded  
255 that while both strains are robust in reducing  $\text{BOD}_5$  and  $\text{PO}_4^{3-}$  levels, the warm strain coupled with  
256 higher temperature is more efficient in reducing  $\text{NH}_4^+\text{-N}$  contents. Hence, selection of the cold  
257 strain and the associated operation conditions need to be further optimized to ensure reliable and  
258 efficient year-round algal wastewater treatment. For example, strategies such as increasing initial  
259 algae cell concentration, micro-nutrient supplementation, or improved solar heat retention are  
260 expected to enhance the treatment performance.<sup>5,32</sup>

261 As for the fed batch experiment (Warm-FB), all three target contaminants were reduced to  
262 the discharge standards within 2–3 days during the five repeated treatment cycles over a 20-day  
263 period (**Figure 2** and Table S1 in the ESI). This shows further improvement from batch treatment  
264 experiments with the same strain (3–4 days based on this study and literature<sup>5</sup>). Therefore, it is  
265 expected that the cold and transitional season treatment performance can also be improved by  
266 switching to the fed-batch treatment mode. In general, these results indicate that that a single-stage  
267 algal wastewater treatment system can be potentially engineered utilizing *G. sulphuraria* to serve  
268 as an alternative to the current secondary treatment systems, particularly in hot and sunny regions  
269 suitable for the warm strain CCMEE 5587.1.



270

271 **Figure 2.** Characteristics of primary clarified municipal wastewater before and after treatment  
 272 with mixotrophic algal species *G. sulphuraria*. Though the treatment experiment for Warm-B was  
 273 conducted for 10 days, all discharge standards were met within 4 days; treatment for Warm-FB  
 274 was conducted for 5 cycles over a 20-day period and each cycle lasted 2–3 days (depending on  
 275 time needed to reach discharge standards). Levels of BOD<sub>5</sub> (mg O<sub>2</sub>·L<sup>-1</sup>), NH<sub>4</sub><sup>+</sup>-N (mg N·L<sup>-1</sup>), and  
 276 PO<sub>4</sub><sup>3-</sup> (mg·L<sup>-1</sup>) are shown for batch test at cold (Cold-B), transitional (Trans-B), and warm (Warm-  
 277 B) seasons, and a fed-batch test at warm season (Warm-FB). Red dashed lines denote discharge  
 278 standards; error bars show max/min values observed for duplicate BOD<sub>5</sub> tests, and standard  
 279 deviations for triplicate NH<sub>4</sub><sup>+</sup>-N and PO<sub>4</sub><sup>3-</sup> tests.

### 280 3.2 Algal biomass properties and HTL yields

281 The harvested algal biomass exhibited characteristics typical of wastewater algae with much  
 282 lower lipid but higher ash contents compared to freshwater/saltwater-cultivated species.<sup>33–36</sup> At the  
 283 same time, distinctive variations were observed among biomass harvested in different seasons

284 (Table 1 and Table S2 in the ESI). Specifically, the Cold-B biomass had the lowest lipid (1.3  
 285 dw%) and protein (30.6 dw%) contents and the highest carbohydrate (27.5 dw%) and ash (29.2  
 286 dw%) contents, which were expected to result in the lowest biocrude yields but higher co-product  
 287 yields.<sup>14</sup> The Trans-B biomass, on the other hand, possessed the highest lipid (7.3 dw%) and  
 288 protein (56.1 dw%) contents and lowest ash (10.3 dw%) content, and therefore was expected to  
 289 yield the most biocrude and lower quantities of co-products. Biomass from Warm-B and Warm-  
 290 FB experiments were similar in composition, with lipid, protein, and ash contents between Cold-  
 291 B and Trans-B, and much lower carbohydrate contents (11.1 and 9.8 dw% for Warm-B and Warm-  
 292 FB, respectively). The resemblance between Warm-B and Warm-FB batches support the  
 293 feasibility of operating the algal wastewater treatment systems with partial biomass recirculation  
 294 and shorter retention time. In addition, as the Trans-B was a polyculture of the cold and warm  
 295 strains but possessed characteristics that were more favorable for HTL conversion, the current  
 296 treatment conditions are likely to be suitable for producing high-quality biomass during  
 297 transitional period only; further optimization will be needed to improve biomass characteristics  
 298 during warm and cold seasons. As it has been reported that algal biomass properties can be  
 299 regulated by adjusting operating conditions while maintaining robust nutrient removal,<sup>4</sup> it follows  
 300 that further optimization of the reactor system conditions can potentially lead to cold and warm  
 301 season biomass with similar properties as the Trans-B that is favorable for HTL conversion.

302 **Table 1** Algal biomass properties and HTL yields (dw%)<sup>a</sup>

		Cold-B	Trans-B	Warm-B	Warm-FB
Biochemical composition	Lipid	1.3±0.7	7.3±0.3	5.3±0.5	4.8±0.03
	Protein <sup>b</sup>	30.6±0.3	56.1 <sup>c</sup>	45.7±0.1	51.6 <sup>c</sup>
	Carbohydrate	27.5±1.0	21.4±1.7	11.1±0.5	9.8±1.9
	Ash	29.2±0.3	10.3±0.1	17.3±0.2	17.0±0.1
HTL yields (300°C)	Biocrude	7.6±0.4	27.5±3.2	13.2±1.0	15.5±1.7
	TDS <sup>d</sup>	9.6±0.9	23.2±0.6	25.4±0.2	24.1±2.7
	Gas	23.7±2.5	17.1±1.7	21.5±2.6	16.7±1.8

	Biochar	43.0±4.6	12.0±0.5	23.8±1.5	26.0±1.3
	Biocrude	13.5±2.0	33.9±0.6	26.6±0.2	21.4±2.5
HTL yields (350°C)	TDS <sup>d</sup>	10.8±0.5	13.4±0.2	15.1±0.9	14.8±2.5
	Gas	19.9±0.7	21.1±0.8	29.1±4.3	24.3±4.6
	Biochar	39.0±3.2	10.5±0.5	22.9±1.2	26.9±1.6

<sup>a</sup> Results represent average±max/min of duplicate analysis; errors for volatile oxygen contents and higher heating values (HHVs) calculated by error propagation methods.

<sup>b</sup> Calculated by using  $6.25 \times$  feedstock nitrogen contents.<sup>23</sup>

<sup>c</sup> No error value because duplicate analysis yielded the same results.

<sup>d</sup> Aqueous total dissolved solids.

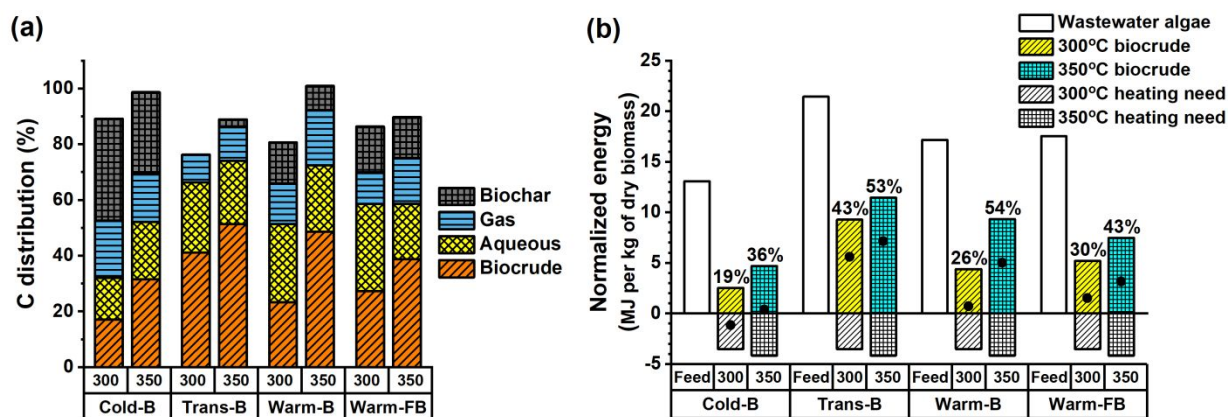
303 HTL experiments were conducted to provide accurate information on yields and characteristics  
 304 of the HTL products, which had been identified as critical impactors toward overall economic  
 305 performance.<sup>8,9,17</sup> Reactions were carried out using 20 dw% algal slurries, which has been reported  
 306 as a reasonable tradeoff between the capital cost for larger HTL system (due to more dilute  
 307 biomass), the operating cost for dewatering biomass to a higher solid content, and the heating  
 308 need.<sup>8</sup> Two previously reported optimum reaction temperatures (300 and 350°C)<sup>37,38</sup> were  
 309 examined to determine the more suitable one for this application. Distinguishable product patterns  
 310 were observed as a result of varying biomass properties and reaction temperatures (**Table 1** and  
 311 Tables S2–S4 in the ESI). As expected from the trends in feedstock lipid and protein contents,  
 312 processing biomass from Trans-B yielded the most HTL biocrude (27.5 dw% at 300°C and 33.9  
 313 dw% at 350°C, respectively), followed by Warm-B and Warm-FB (13.2 and 15.5 dw% at 300°C,  
 314 26.6 and 21.4 dw% at 350°C, respectively), and lowest yields for the low-lipid, low-protein Cold-B  
 315 biomass (7.6 dw% at 300°C and 13.5 dw% at 350°C, respectively). For Trans-B, Warm-B, and  
 316 Warm-FB, yields of biocrude were higher or comparable to other HTL products, but biochar was  
 317 the dominant product for Cold-B with yields of 43.0 dw% at 300°C and 39.0 dw% at 350°C due  
 318 to its high carbohydrate (27.5 dw%) and ash (29.2 dw%) contents. As for the effects of  
 319 temperature, HTL at 350°C generated more biocrude and gaseous products and less aqueous total  
 320 dissolved solids (TDS) and biochar products than 300°C, both of which were in agreement with

321 previously reported trends.<sup>37,39</sup> Although higher HTL reaction temperature is demonstrated to  
322 promote biocrude formation (critical to process economics<sup>7,8</sup>), greater energy inputs are required  
323 to heat the algal slurries to these conditions. Hence, there are tradeoffs associated with processing  
324 temperature selection, which are discussed in following sections.

### 325 **3.3 Energy recovery**

326 Distribution of carbon among HTL products can reflect the allocation of initial energy in the  
327 wastewater algae feedstock, and substantial variations were found for different batches and HTL  
328 temperatures (**Figure 3a**). In general, 17.0–51.4% of the feedstock carbon was transferred to the  
329 desired biocrude products. This wide range results primarily from differences in biocrude yields  
330 since there were only small variations in carbon contents of the different biocrudes (70.2–73.5%  
331 C). HTL was most efficient in transferring carbon from the Trans-B biomass into biocrude, with  
332 41.2 and 51.4% of feedstock's carbon converting into biocrude products at 300 and 350°C,  
333 respectively. In contrast, only 17.0% (300°C) and 31.5% (350°C) of the carbon in the Cold-B  
334 biomass transferred into the HTL biocrude product; a greater fraction of the carbon in this  
335 feedstock transferred to the biochar product (up to 36.5%). 15.0–31.2% of the carbon ended up in  
336 aqueous co-products, representing a non-negligible portion of the feedstock energy. Though not  
337 directly upgradable to liquid biofuels, aqueous organic compounds can be recovered as  
338 energetically valuable fuel gas products (mostly CH<sub>4</sub> and H<sub>2</sub>) by CHG, which can be used for  
339 onsite co-generation of heat (for reactor heating)/electricity and catalytic upgrading of biocrude to  
340 refined fuel products.<sup>8,30,31</sup> Other technologies like anaerobic digestion<sup>40</sup> and microbial electrolysis  
341 cells<sup>41</sup> can also be used to recover the energy embedded in aqueous organics as biogas or H<sub>2</sub>.  
342 Lastly, 10.0–20.6% of the feedstock carbon was converted to gaseous products during the HTL  
343 conversion. As the gaseous products are predominantly CO<sub>2</sub><sup>31</sup> and of little energetic value, they

344 can be recycled to support biomass growth.<sup>8</sup> With regard to reaction temperature, it was found that  
 345 more carbon from the feedstock could be transferred to biocrudes at 350°C as a result of increased  
 346 yields and higher biocrude carbon contents observed at this temperature. At the same time,  
 347 increasing temperature reduced the level of carbon that ended up in the biochar products, a result  
 348 of both the lower biochar yields and biochar carbon contents. It follows that performing HTL at  
 349 the higher temperature is advantageous for improving feedstock conversion and energy recovery  
 350 in the biocrude product.



351

352 **Figure 3.** Carbon distribution between HTL products (a) and energy normalized to 1 kg of dry  
 353 algae (b). Four batches of harvested *G. sulphuraria* (Cold-B, Trans-B, Warm-B, and Warm-FB)  
 354 and two HTL reaction temperatures (300 and 350°C) were included. In (a), carbon content of  
 355 biochar for the Trans-B at 300°C could not be determined due to the small amount of sample  
 356 generated. In (b), open columns show feedstock energy; colored and hatched columns show energy  
 357 in biocrude generated from 1 kg of dry algae; uncolored hatched columns show heating needs;  
 358 black dots show the net energy that could be recovered from biocrude after subtraction of heating  
 359 need; data labeled at the top of columns indicate energy recovery of biocrude (percentage of  
 360 feedstock energy that can be recovered in biocrude, calculated on dry weight basis). Results are  
 361 average of duplicate experiments and detailed data with uncertainties can be found in Tables S2–  
 362 S4 in the ESI.

363 To give a straightforward illustration of the energy flows during HTL reactions, energy in algal  
 364 biomass, HTL biocrudes, and the amount required to heat the algal slurries to each reaction  
 365 temperature were calculated (**Figure 3b**). For 1 kg of dry biomass, the Trans-B biomass had the

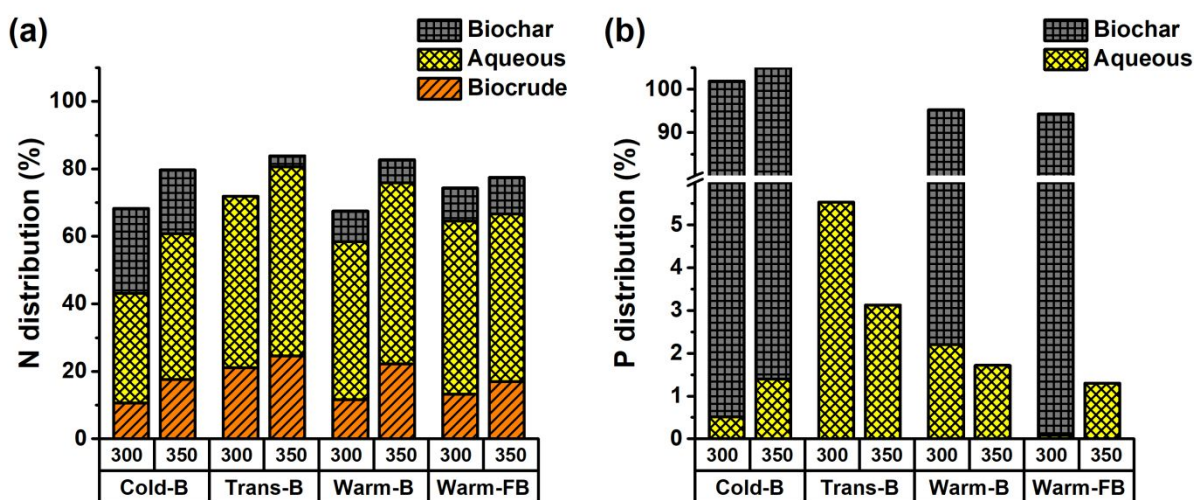
366 highest energy content ( $21.4 \text{ MJ}\cdot\text{kg}^{-1}$  on dry weight basis), followed by the biomass for Warm-FB  
367 ( $17.5 \text{ MJ}\cdot\text{kg}^{-1}$ ) and Warm-B ( $17.2 \text{ MJ}\cdot\text{kg}^{-1}$ ), all of which were comparable to previously reported  
368 freshwater-cultivated algal biomass.<sup>14,42</sup> The biomass from Cold-B had a lower energy content  
369 ( $13.1 \text{ MJ}\cdot\text{kg}^{-1}$ ) due to its high ash content, which is not uncommon among wastewater algae.<sup>33,35</sup>  
370 For the HTL reactions, it was estimated that the heating needs (3.5 and 4.2 MJ per kg of dry algae  
371 for 300 and 350°C, respectively) represented 16.5–31.9% of the energy embedded in the starting  
372 biomass. The generated biocrudes would contain 2.5–11.5 MJ of energy (colored columns in  
373 **Figure 3b**), representing 19.2–54.3% of the energy embedded in the initial algae (data labeled in  
374 **Figure 3b**). Subtraction of the heating needs revealed the net amounts of energy that could be  
375 recovered in the form of biocrude (black dots and labels in **Figure 3b**), which followed the order  
376 of Trans-B > Warm-B and Warm-FB > Cold-B, and 350°C > 300°C. Thus, although HTL  
377 conversion at 350°C required more input energy, it would be more than offset by the increased  
378 biocrude yield and HHV. Notably, for HTL at 350°C, all four batches of algae generated biocrudes  
379 containing more energy than heating needs, supporting the feasibility of HTL-based conversion  
380 process.

### 381 **3.4 Nutrient recycling**

382 Recovery of nutrients (most importantly nitrogen and phosphorus<sup>43–45</sup>) in conversion process  
383 is another important aspect for economics and sustainability of the overall system,<sup>46,47</sup> which can  
384 vary greatly over different algal biomass<sup>14</sup> but not yet well studied for large-scale systems.<sup>8</sup> **Figure**  
385 **4** shows the distribution of nitrogen and phosphorus within the HTL products observed in this  
386 study. Unlike the distribution of carbon, which varied widely between different biomass feedstocks  
387 (e.g., Cold-B versus Trans-B) and products (e.g., biocrudes versus biochars), much less variation  
388 was observed for the distribution of nitrogen (**Figure 4a**). The largest fraction of feedstock

389 nitrogen ended up in the aqueous co-products, close to or exceeding 50% for most reactions. Even  
390 aqueous products of the Cold-B, where yields were less than 30% of biochar products', contained  
391 most of the feedstock nitrogen among all products. This finding was consistent with earlier reports  
392 on HTL of algal biomass<sup>14,48</sup> and revealed a strong tendency of nitrogen-containing compounds to  
393 partition into the aqueous phase. Aside from aqueous products, a substantial fraction of the  
394 feedstock nitrogen also transferred into the biocrude and biochar products (10.7–24.6% for  
395 biocrudes and 3.3–25.2% for biochars). Similar to the case of carbon, these observed variations  
396 resulted mostly from the distinctive product yields rather than nitrogen contents of the different  
397 products, which were found to be narrowly constrained (6.1–7.0% for biocrudes and 2.2–3.3% for  
398 biochars). On the impacts of reaction temperature, generally more nitrogen was directed to  
399 biocrude and aqueous products and less to biochar products at 350°C. It should be noted that the  
400 increase in nitrogen distribution to biocrudes resulted from the increase in biocrude yields rather  
401 than higher biocrude nitrogen contents. In fact, nitrogen contents of the biocrudes generated at  
402 350°C (6.1–6.5%) were found to be slightly lower than biocrudes generated at 300°C (6.4–7.0%),  
403 which is preferred, as elevated nitrogen content is detrimental to biocrude quality, negatively  
404 influencing refined fuel yields from hydrotreating processes.<sup>8</sup> Aqueous nitrogenous constituents  
405 mainly existed in the form of  $\text{NH}_4^+$  and organonitrogen compounds,<sup>49</sup> and substantial increases in  
406 aqueous  $\text{NH}_4^+$ -N contents were observed with increasing HTL temperature (3350–8450  $\text{mg N}\cdot\text{L}^{-1}$   
407 at 350°C versus 1980–4870  $\text{mg N}\cdot\text{L}^{-1}$  at 300°C). This can be attributed to the further degradation  
408 of organonitrogen compounds (both in the biocrude and aqueous products) at more severe reaction  
409 conditions, which is preferred because  $\text{NH}_4^+$  can be more readily recovered for production of  
410 commercial fertilizers (e.g., ammonium sulfate) or recycled for algae cultivation.<sup>46,50,51</sup>

411 Phosphorus contents of the biochar products could only be directly determined for half of the  
 412 experiments (because of the small amounts of biochar generated during some reactions), but  
 413 analyses of the aqueous products (all batches) and available biochar products revealed a clear  
 414 tendency for phosphorus species to be incorporated into the solid phase products (**Figure 4b**),  
 415 likely in the form of polyvalent phosphate salts (e.g., calcium phosphate).<sup>49</sup> For all experiments,  
 416 around or less than 5% of the feedstock phosphorus transferred into the aqueous phase after HTL  
 417 reaction, compared to 93.1–104.6% in the biochar products (phosphorus contents of biocrude and  
 418 gaseous products were assumed to be negligible<sup>49</sup>). The strong tendency for phosphorus  
 419 distribution to the biochar was even more evident for reactions conducted at 350°C, where aqueous  
 420 phosphorus species only accounted for 1.3–3.1% of the phosphorus originally present in the  
 421 feedstock. The diversion of almost all phosphorus to biochar is advantageous for subsequent  
 422 recovery of energy from the HTL aqueous products through catalytic processes (e.g., CHG) where  
 423 phosphorus can poison and deactivate catalysts.<sup>52,53</sup> Additionally, the concentration of phosphorus  
 424 in biochar is beneficial for the direct use of biochar as a soil amendment and fertilizer,<sup>54,55</sup> or as a  
 425 source material for production of other phosphorus-containing fertilizers.<sup>43,46</sup>

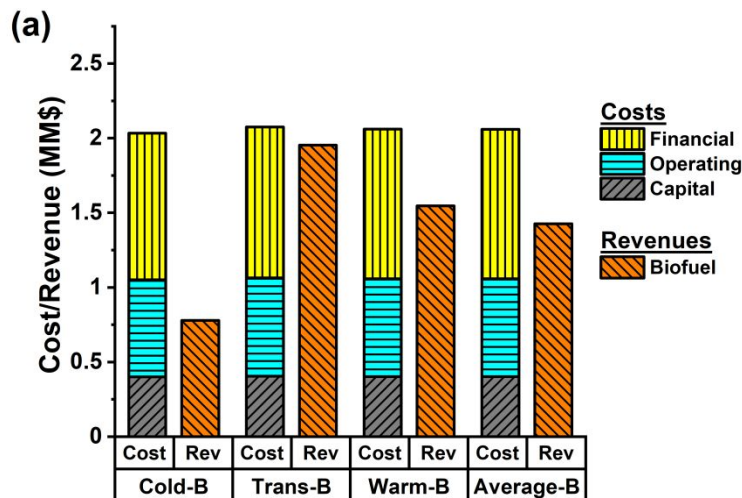


426

427 **Figure 4.** Nitrogen (a) and phosphorus (b) distributions between HTL products. Four batches of  
428 harvested *G. sulphuraria* (Cold-B, Trans-B, Warm-B, and Warm-FB) and two HTL reaction  
429 temperatures (300 and 350°C) were included. Biochar nitrogen content of the Trans-B at 300°C,  
430 and phosphorus contents of Trans-B, Warm-B, and Warm-FB batches at 350°C could not be  
431 measured due to small quantities of biochar generated. Results are average of duplicate  
432 experiments and detailed data with uncertainties can be found in Tables S2–S4 in the ESI.

### 433 3.5 System evaluation and path forward

434 Following HTL experiments, economic analysis was conducted to compare the costs and  
435 revenues of the conversion processes (**Figure 5** and Tables S5 and S6 in the ESI). For all batches,  
436 a similar cost of 2.0–2.1 million dollars per year (MM \$·yr<sup>-1</sup>) was calculated (annualized results  
437 assuming year-round operation with only the respective strain, adjusted to 25.6 TPD). This was  
438 expected as properties of algae had minor effects on size of the major equipment (therefore total  
439 capital cost).<sup>56</sup> However, much larger variations were observed when comparing revenues derived  
440 from conversion of these wastewater algae. While less than 0.8 MM \$·yr<sup>-1</sup> was calculated for Cold-  
441 B due to the low biofuel yields, 1.6 MM \$·yr<sup>-1</sup> was expected for Warm-B and 2.0 MM \$·yr<sup>-1</sup> for  
442 Trans-B. Assuming a year-round operation with a third of Cold-B, Trans-B, and Warm-B each, an  
443 average revenue (Average-B) of 1.4 MM \$·yr<sup>-1</sup> was predicted. Overall, annual loss of 0.1–1.3  
444 MM\$·yr<sup>-1</sup> was predicted and was consistent with existing literature. Previous research concluded  
445 that in order for the plant to break even, the minimum selling price of HTL-derived biofuel needs  
446 to be \$4.49–32.60 gal<sup>-1</sup> with an average of \$10.23 gal<sup>-1</sup>.<sup>7,28,57–59</sup> Assuming 70% of the costs were  
447 attributed to feedstock,<sup>29</sup> the conversion process accounted for \$1.35–9.78 gal<sup>-1</sup> with an average of  
448 \$3.07 gal<sup>-1</sup>, higher than the value of \$2.79 gal<sup>-1</sup> used in this study, thus leading to negative net  
449 revenues. For wastewater algae examined in this study, biofuel should be priced at \$3.10–6.47  
450 gal<sup>-1</sup> for the plant to break even, which is in the range reported in literature.

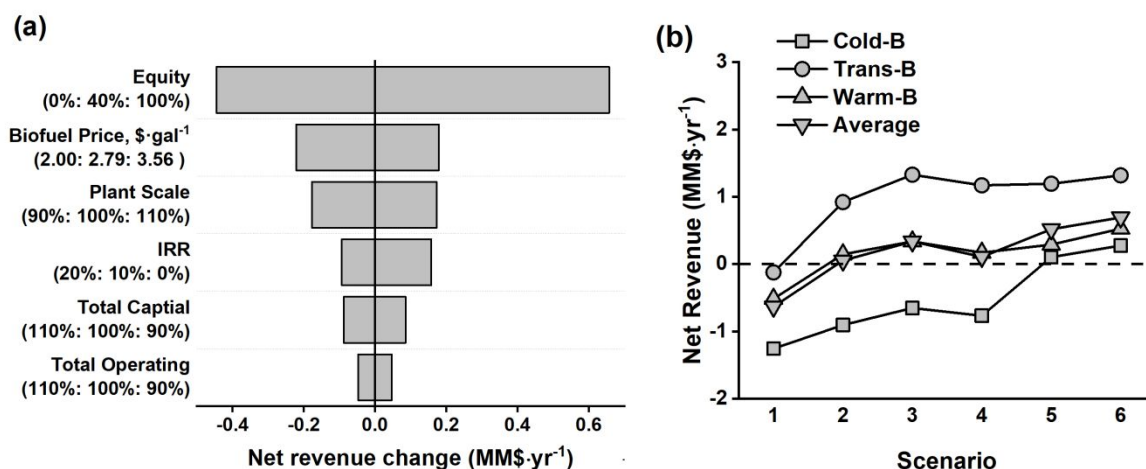


451

452 **Figure 5.** Process economic analysis for harvested *G. sulphuraria*. Results of Cold-B, Trans-B,  
 453 and Warm-B were calculated using the respective experiment data (350°C HTL conversion) as  
 454 inputs of the model described in a previous study;<sup>7</sup> results for batch Average-B were calculated  
 455 using the average HTL results of Cold-B, Trans-B, and Warm-B as model inputs. Warm-FB gave  
 456 similar results as Warm-B thus not presented. Costs/credits from algal treatment of wastewater  
 457 were not included due to lack of large-scale studies on such processes. Detailed cost and revenue  
 458 breakdown can be found in Tables S5 and S6 in the ESI.

459 To characterize the impact from key factors on the overall system, sensitivity and uncertainty  
 460 analyses were conducted for the baseline scenario of Average-B (**Figure 6a**), which better  
 461 represented the composition of wastewater algae that could be harvested from year-round  
 462 operation. Financial cost coming from loan payments was found to be the largest contributor (0.7  
 463 MM \$·yr<sup>-1</sup>), thus changes in project equity would affect the overall cost in the most significant  
 464 way. As biofuel was the only product in the baseline scenario, the system was sensitive to the  
 465 selling price of biofuel, and a  $\sim\pm 0.2$  MM \$·yr<sup>-1</sup> ( $\sim\pm 15\%$  of total revenue) was estimated based on  
 466 the changes of commercial gasoline price over the past 10 years.  $\pm 10\%$  of the baseline plant scale  
 467 would shift the overall economics in a similar way as biofuel price, but if algae from the wastewater  
 468 treatment plant was the only feedstock source (i.e., plant scale decreased to 25.6 TPD, or only  
 469 4.4% of the baseline value), then the total cost would be more than doubled with no changes in  
 470 revenues. This economy of scale reveals the necessity to have central conversion plants for large

471 quantities of feedstocks, and additional feedstock sources should be considered. In fact, a broad  
 472 spectrum of organic materials (e.g., food wastes,<sup>60</sup> manure,<sup>15</sup> waste plastics<sup>61</sup>) can be included as  
 473 HTL is widely applicable. Moreover, as yields and characteristics of HTL products are determined  
 474 by feedstock biochemical compositions (lipid, protein, carbohydrate, and ash contents) rather than  
 475 feedstock type (e.g., algae versus manure), results from this study can be extended to other waste  
 476 biomass with similar properties (e.g., sludge and manure which have low lipid but high ash  
 477 contents).<sup>14</sup> IRR evaluates the attractiveness of the project and 10% has been recommended for  
 478 renewable energy-related projects.<sup>62</sup> An IRR of 0% could increase the revenue by 0.16 MM \$·yr<sup>-1</sup>  
 479 <sup>1</sup>, but investors would not be interested in this project considering inflation and project risk. Total  
 480 capital and total operating costs were expected to have smaller effects (<0.1 MM \$·yr<sup>-1</sup>) and the  
 481 effects were symmetric for minimum and maximum boundaries. Overall, as the baseline scenario  
 482 of Average-B had a negative revenue of -0.63 MM \$·yr<sup>-1</sup>, which was larger than the scales of  
 483 changes that could be brought by these factors other than 100% equity, the project was not likely  
 484 to be profitable under the current design.



485

486 **Figure 6.** (a) Sensitivity and uncertainty analyses for Average-B in **Figure 5**; examined factors  
 487 included percentage of project equity, selling price of biofuel, scale of the biorefinery plant,  
 488 internal rate of return (IRR), total capital investment, and total operating cost. (b) Changes in net

489 revenues under different scenarios. Scenario 1 was the baseline scenario in **Figure 5**; Scenario 2  
490 included revenue from ammonium sulfate; Scenario 3 included revenues from both ammonium  
491 sulfate and struvite; Scenario 4 included revenues from both ammonium sulfate and struvite, and  
492 assumed wastewater algae were harvested at their peak storage level (maximum lipid and  
493 carbohydrate contents); Scenario 5 and 6 included revenues from both ammonium sulfate and  
494 struvite, and assumed carbohydrates in algae were hydrolyzed and fermented to ethanol, lipids in  
495 algae were extracted and hydrotreated to green diesel prior to HTL conversion based on model  
496 in<sup>29</sup>, Scenario 5 was calculated for the baseline composition and Scenario 6 was calculated for the  
497 peak-storage composition.<sup>29</sup> Detailed cost breakdown can be found in Tables S5–S7 in the ESI.

498 While revenues from biofuels alone could not cover the anticipated costs of these conversion  
499 processes, inclusion of nutrient co-products (ammonium sulfate and struvite) could potentially flip  
500 the balance sheet. Specifically, 0.4–1.0 MM \$·yr<sup>-1</sup> in additional revenue was predicted for  
501 ammonium sulfate, which was enough to bring net revenues for Trans-B, Warm-B, and Average-  
502 B above 0 (Scenario 2 in **Figure 6b** and Tables S5 and S6 in the ESI), and inclusion of struvite  
503 would add another 0.2–0.4 MM \$·yr<sup>-1</sup> in revenue (Scenario 3 in **Figure 6b** and Tables S5 and S6  
504 in the ESI). Moreover, current ammonium sulfate yields were based on NH<sub>4</sub><sup>+</sup>-N contents of HTL  
505 aqueous products. Since the subsequent CHG step can convert almost all other non-NH<sub>4</sub><sup>+</sup> N-  
506 containing species in HTL aqueous products (e.g., organic nitrogen species) to NH<sub>4</sub><sup>+</sup>-N,<sup>8,9,31</sup>  
507 revenues from ammonium sulfate could be >50% higher than current estimates. Though costs of  
508 generating these nutrient co-products could not be calculated at this stage, these processes were  
509 conducted at much milder conditions than the hydrothermal processes, so costs are expected to be  
510 relatively small compared to those producing fuels. Overall, revenues from these nutrient co-  
511 products were 55–78% of the biofuel sales and demonstrated that nutrient recovery was not only  
512 a necessity for environmental sustainability of algal bioproducts,<sup>43–45</sup> but also important for  
513 economic considerations. Since algae samples used in this study were harvested after ≥10 days  
514 when part of the storage compounds (lipids and carbohydrates) had been consumed, additional  
515 evaluations were conducted for algae at their peak storage levels (day 4 of growth based on<sup>18</sup>,

516 sufficient for Warm-B and Warm-FB to meet discharge standards<sup>20</sup>). Composition of algae were  
517 simulated based on previously reported growth profile<sup>18</sup> and were characterized by higher lipid  
518 and carbohydrate contents but lower protein contents (3.1–13.7% lipids, 40.3–62.5% proteins, and  
519 23.8–56.6% carbohydrates for peak-storage scenario versus 2.1–8.6% lipids, 51.5–71.5% proteins,  
520 and 17.9–46.3% carbohydrates for baseline scenario, all corrected to 100% ash-free dry weight  
521 basis, ash contents were assumed to be the same). However, these changes in composition led to  
522 0.12–0.23 MM \$·yr<sup>-1</sup> decrease in revenues (Scenario 4 in **Figure 6b** and Table S7 in the ESI),  
523 which was due to the tradeoffs between different products. As HTL is not efficient in converting  
524 carbohydrates to fuels (16% carbohydrate-to-fuel efficiency versus 34% for proteins and 65% for  
525 lipids),<sup>29</sup> the major increase in carbohydrate contents and decrease in protein contents outweighed  
526 benefits from the minor increase in lipid contents, leading to reduction in fuel yields. Moreover,  
527 lower protein contents also led to less ammonium in HTL aqueous product that could be recovered  
528 as ammonium sulfate. Alternatively, component-specific conversion process other than HTL could  
529 be incorporated to improve biomass-to-fuel efficiency and therefore overall revenues. For  
530 example, hybrid system featuring fermentation of carbohydrates to ethanol and  
531 extraction/hydrotreating of lipids to green diesel prior to HTL conversion has been proposed, and  
532 it has been demonstrated with freshwater algae to increase carbohydrate-to-fuel efficiency from  
533 16% to 75% and lipid-to-fuel efficiency from 65% to 79% (compared to HTL alone).<sup>29</sup> Assuming  
534 the same conversion efficiency, substantial increases in net revenues compared to HTL alone could  
535 be achieved for Cold-B (0.8 MM \$·yr<sup>-1</sup> for the baseline scenario and 1.0 MM \$·yr<sup>-1</sup> for the peak-  
536 storage scenario, respectively) with similar net revenues for Trans-B and Warm-B (Scenarios 5  
537 and 6 in **Figure 6b** and Table S7 in the ESI, changes in costs included).<sup>29</sup> On average, these  
538 changes led to increase of 0.2 MM \$·yr<sup>-1</sup> for the baseline scenario and 0.6 MM \$·yr<sup>-1</sup> for the peak-

539 storage scenario, demonstrating the benefit of more efficient conversion of individual components,  
540 especially for carbohydrates. This application of hybrid system was particularly relevant for Cold-  
541 B, whose low lipid and high carbohydrate contents led to negative net revenues even when nutrient  
542 co-products were considered, and the much smaller differences in net revenues between different  
543 batches would allow steadier year-round operation. However, more research should be conducted  
544 in the future to obtain the experimental biomass-to-fuel efficiency for wastewater algae.

545 When viewed from a systems level, this study revealed the underlying connections between  
546 treatment and conversion processes and present the significant effects of the algal strains and  
547 operating modes on treated water quality, properties of the harvested algae, and energy and nutrient  
548 recoveries thereof. While the warm strain was found to be most effective in wastewater treatment,  
549 biomass recovered from the polyculture transitional batch generated the most valuable products  
550 and was expected to have the highest profit. This highlights the tradeoffs that can exist between  
551 treatment efficacy and downstream energy recovery and suggest a need to customize operating  
552 strategies to each season. For example, higher initial algae concentration, micro-nutrient  
553 supplementation, fed-batch operating mode, etc. can be considered to improve the removal of  
554  $\text{NH}_4^+\text{-N}$  in cold and transitional seasons, and treatment time can be shortened for the warm season  
555 due to the higher contaminant removal rate. In addition to treatment operating decisions, energy  
556 and nutrient recoveries can be greatly improved by optimizing conversion conditions and system  
557 configuration. Negative impacts resulting from the elevated ash contents algal biomass (e.g.,  
558 reduced biocrude yields and higher biochar yields) can be alleviated, to a degree, by increasing the  
559 HTL reaction severity, where higher biocrude yields and nutrient recovery in desired products  
560 were observed. More importantly, as wastewater algae are characterized by high carbohydrate  
561 contents that cannot be efficiently converted by HTL, application of hybrid systems with

562 component-specific conversion techniques can lead to substantial improvement in economics  
563 performance. Therefore, treatment experiments with varying solid residence time should be  
564 conducted to establish dynamic contaminant removal and algae composition profile, therefore  
565 recognizing the optimal time for meeting discharge standards while maintaining high levels of  
566 storage compounds in algal biomass for greater biofuel yields. Overall, this work shows the  
567 potential of algal wastewater treatment systems for energy and nutrient recovery, which are  
568 promising in turning wastewater treatment plants into profitable water resource recovery facilities.

### 569 **Conflicts of interest**

570 There are no conflicts of interest to declare.

### 571 **Acknowledgements**

572 This work was supported by National Science Foundation (NSF) through the NSF Engineering  
573 Research Center for Reinventing the Nation's Urban Water Infrastructure (ReNUWIt; EEC-  
574 1028968), and NSF awards CBET-1555549 and CBET-1438667.

575 **References**

- 576 (1) McCarty, P. L.; Bae, J.; Kim, J. Domestic Wastewater Treatment as a Net Energy Producer–  
577 Can This Be Achieved? *Environ. Sci. Technol.* **2011**, *45* (17), 7100–7106.  
578 <https://doi.org/10.1021/es2014264>.
- 579 (2) Gao, H.; Scherson, Y. D.; Wells, G. F. Towards Energy Neutral Wastewater Treatment:  
580 Methodology and State of the Art. *Environ. Sci. Process. Impacts* **2014**, *16* (6), 1223–1246.  
581 <https://doi.org/10.1039/C4EM00069B>.
- 582 (3) Li, W.-W.; Yu, H.-Q.; Rittmann, B. E. Chemistry: Reuse Water Pollutants. *Nat. News* **2015**,  
583 *528* (7580), 29. <https://doi.org/10.1038/528029a>.
- 584 (4) Gardner-Dale, D. A.; Bradley, I. M.; Guest, J. S. Influence of Solids Residence Time and  
585 Carbon Storage on Nitrogen and Phosphorus Recovery by Microalgae across Diel Cycles.  
586 *Water Res.* **2017**, *121*, 231–239. <https://doi.org/10.1016/j.watres.2017.05.033>.
- 587 (5) Henkanatte-Gedera, S. M.; Selvaratnam, T.; Karbakhshravari, M.; Myint, M.;  
588 Nirmalakhandan, N.; Van Voorhies, W.; Lammers, P. J. Removal of Dissolved Organic  
589 Carbon and Nutrients from Urban Wastewaters by *Galdieria Sulphuraria*: Laboratory to  
590 Field Scale Demonstration. *Algal Res.* **2017**, *24*, Part B, 450–456.  
591 <https://doi.org/10.1016/j.algal.2016.08.001>.
- 592 (6) Selvaratnam, T.; Henkanatte-Gedera, S. M.; Muppaneni, T.; Nirmalakhandan, N.; Deng, S.;  
593 Lammers, P. J. Maximizing Recovery of Energy and Nutrients from Urban Wastewaters.  
594 *Energy* **2016**, *104*, 16–23. <https://doi.org/10.1016/j.energy.2016.03.102>.
- 595 (7) Leow, S.; Shoener, B. D.; Li, Y.; DeBellis, J. L.; Markham, J.; Davis, R.; Laurens, L. M.  
596 L.; Pienkos, P. T.; Cook, S. M.; Strathmann, T. J.; et al. A Unified Modeling Framework to  
597 Advance Biofuel Production from Microalgae. *Environ. Sci. Technol.* **2018**, *52* (22), 13591–  
598 13599. <https://doi.org/10.1021/acs.est.8b03663>.
- 599 (8) Jones, S. B.; Zhu, Y.; Anderson, D. B.; Hallen, R. T.; Elliott, D. C.; Schmidt, A. J.; Albrecht,  
600 K. O.; Hart, T. R.; Butcher, M. G.; Drennan, C.; et al. *Process Design and Economics for*  
601 *the Conversion of Algal Biomass to Hydrocarbons: Whole Algae Hydrothermal*  
602 *Liquefaction and Upgrading*; PNNL-23227; Pacific Northwest National Laboratory  
603 (PNNL), Richland, WA (US), 2014.
- 604 (9) Li, Y.; Tarpeh, W. A.; Nelson, K. L.; Strathmann, T. J. Quantitative Evaluation of an  
605 Integrated System for Valorization of Wastewater Algae as Bio-Oil, Fuel Gas, and Fertilizer  
606 Products. *Environ. Sci. Technol.* **2018**, *52* (21), 12717–12727.  
607 <https://doi.org/10.1021/acs.est.8b04035>.
- 608 (10) Davis, R.; Markham, J.; Kinchin, C.; Grundl, N.; Tan, E. C. D.; Humbird, D. *Process Design*  
609 *and Economics for the Production of Algal Biomass: Algal Biomass Production in Open*  
610 *Pond Systems and Processing Through Dewatering for Downstream Conversion*; National  
611 Renewable Energy Laboratory (NREL), Golden, CO., 2016.
- 612 (11) Menger-Krug, E.; Niederste-Hollenberg, J.; Hillenbrand, T.; Hiessl, H. Integration of  
613 Microalgae Systems at Municipal Wastewater Treatment Plants: Implications for Energy  
614 and Emission Balances. *Environ. Sci. Technol.* **2012**, *46* (21), 11505–11514.  
615 <https://doi.org/10.1021/es301967y>.
- 616 (12) Xin, C.; Addy, M. M.; Zhao, J.; Cheng, Y.; Cheng, S.; Mu, D.; Liu, Y.; Ding, R.; Chen, P.;  
617 Ruan, R. Comprehensive Techno-Economic Analysis of Wastewater-Based Algal Biofuel  
618 Production: A Case Study. *Bioresour. Technol.* **2016**, *211*, 584–593.  
619 <https://doi.org/10.1016/j.biortech.2016.03.102>.

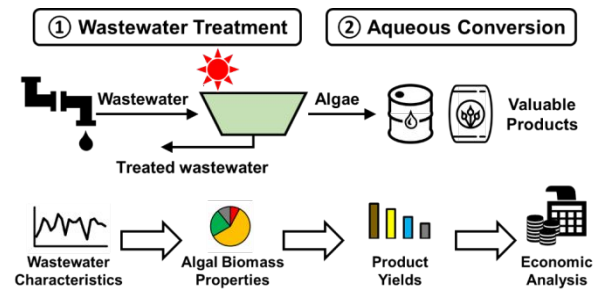
- 620 (13) Ranganathan, P.; Savithri, S. Techno-Economic Analysis of Microalgae-Based Liquid Fuels  
621 Production from Wastewater via Hydrothermal Liquefaction and Hydroprocessing.  
622 *Bioresour. Technol.* **2019**, *284*, 256–265. <https://doi.org/10.1016/j.biortech.2019.03.087>.
- 623 (14) Li, Y.; Leow, S.; Fedders, A. C.; Sharma, B. K.; Guest, J. S.; Strathmann, T. J. Quantitative  
624 Multiphase Model for Hydrothermal Liquefaction of Algal Biomass. *Green Chem.* **2017**, *19*  
625 (4), 1163–1174. <https://doi.org/10.1039/C6GC03294J>.
- 626 (15) Chen, W.-T.; Zhang, Y.; Zhang, J.; Schideman, L.; Yu, G.; Zhang, P.; Minarick, M. Co-  
627 Liquefaction of Swine Manure and Mixed-Culture Algal Biomass from a Wastewater  
628 Treatment System to Produce Bio-Crude Oil. *Appl. Energy* **2014**, *128*, 209–216.  
629 <https://doi.org/10.1016/j.apenergy.2014.04.068>.
- 630 (16) Cheng, F.; Cui, Z.; Chen, L.; Jarvis, J.; Paz, N.; Schaub, T.; Nirmalakhandan, N.; Brewer,  
631 C. E. Hydrothermal Liquefaction of High- and Low-Lipid Algae: Bio-Crude Oil Chemistry.  
632 *Appl. Energy* **2017**, *206* (Supplement C), 278–292.  
633 <https://doi.org/10.1016/j.apenergy.2017.08.105>.
- 634 (17) Albrecht, K. O.; Zhu, Y.; Schmidt, A. J.; Billing, J. M.; Hart, T. R.; Jones, S. B.; Maupin,  
635 G.; Hallen, R.; Ahrens, T.; Anderson, D. Impact of Heterotrophically Stressed Algae for  
636 Biofuel Production via Hydrothermal Liquefaction and Catalytic Hydrotreating in  
637 Continuous-Flow Reactors. *Algal Res.* **2016**, *14*, 17–27.  
638 <https://doi.org/10.1016/j.algal.2015.12.008>.
- 639 (18) Fedders, A. C.; DeBellis, J. L.; Bradley, I. M.; Sevillano-Rivera, M. C.; Pinto, A. J.; Guest,  
640 J. S. Comparable Nutrient Uptake across Diel Cycles by Three Distinct Phototrophic  
641 Communities. *Environ. Sci. Technol.* **2019**, *53* (1), 390–400.  
642 <https://doi.org/10.1021/acs.est.8b05874>.
- 643 (19) Schönknecht, G.; Chen, W.-H.; Ternes, C. M.; Barbier, G. G.; Shrestha, R. P.; Stanke, M.;  
644 Bräutigam, A.; Baker, B. J.; Banfield, J. F.; Garavito, R. M.; et al. Gene Transfer from  
645 Bacteria and Archaea Facilitated Evolution of an Extremophilic Eukaryote. *Science* **2013**,  
646 *339* (6124), 1207–1210. <https://doi.org/10.1126/science.1231707>.
- 647 (20) Henkanatte-Gedera, S. M.; Selvaratnam, T.; Caskan, N.; Nirmalakhandan, N.; Van  
648 Voorhies, W.; Lammers, P. J. Algal-Based, Single-Step Treatment of Urban Wastewaters.  
649 *Bioresour. Technol.* **2015**, *189*, 273–278. <https://doi.org/10.1016/j.biortech.2015.03.120>.
- 650 (21) Gross, W.; Oesterhelt, C.; Tischendorf, G.; Lederer, F. Characterization of a Non-  
651 Thermophilic Strain of the Red Algal Genus *Galdieria* Isolated from Soos (Czech Republic).  
652 *Eur. J. Phycol.* **2002**, *37* (3), 477–482. <https://doi.org/10.1017/S0967026202003773>.
- 653 (22) U.S. EPA. *SW-846 Test Method 3052: Microwave Assisted Acid Digestion of Siliceous and*  
654 *Organically Based Matrices*; Policies and Guidance; 1996.
- 655 (23) Sosulski, F. W.; Imafidon, G. I. Amino Acid Composition and Nitrogen-to-Protein  
656 Conversion Factors for Animal and Plant Foods. *J. Agric. Food Chem.* **1990**, *38* (6), 1351–  
657 1356. <https://doi.org/10.1021/jf00096a011>.
- 658 (24) Haynes, W. M. *CRC Handbook of Chemistry and Physics, 97th Edition*, 97th ed.; CRC  
659 Press, 2016.
- 660 (25) APHA; AWWA. *Standard Methods for the Examination of Water and Wastewater*, 21st  
661 ed.; American Public Health Association: Washington, D.C., 2005.
- 662 (26) Leow, S.; Witter, J. R.; Vardon, D. R.; Sharma, B. K.; Guest, J. S.; Strathmann, T. J.  
663 Prediction of Microalgae Hydrothermal Liquefaction Products from Feedstock Biochemical  
664 Composition. *Green Chem* **2015**, *17* (6), 3584–3599.  
665 <https://doi.org/10.1039/C5GC00574D>.

- 666 (27) U.S. Energy Information Administration. Annual Energy Outlook  
667 <https://www.eia.gov/outlooks/aeo/> (accessed May 22, 2019).
- 668 (28) Cruce, J. R.; Quinn, J. C. Economic Viability of Multiple Algal Biorefining Pathways and  
669 the Impact of Public Policies. *Appl. Energy* **2019**, *233–234*, 735–746.  
670 <https://doi.org/10.1016/j.apenergy.2018.10.046>.
- 671 (29) Li, Y.; Leow, S.; Dong, T.; Nagle, N. J.; Knoshaug, E. P.; Laurens, L. M. L.; Pienkos, P. T.;  
672 Guest, J. S.; Strathmann, T. J. Demonstration and Evaluation of Hybrid Microalgae  
673 Aqueous Conversion Systems for Biofuel Production. *ACS Sustain. Chem. Eng.* **2019**, *7* (6),  
674 5835–5844. <https://doi.org/10.1021/acssuschemeng.8b05741>.
- 675 (30) Davis, R.; Kinchin, C.; Markham, J.; Tan, E.; Laurens, L. M. L.; Sexton, D.; Knorr, D.;  
676 Schoen, P.; Lukas, J. *Process Design and Economics for the Conversion of Algal Biomass*  
677 *to Biofuels: Algal Biomass Fractionation to Lipid- and Carbohydrate-Derived Fuel*  
678 *Products*; NREL/TP-5100-62368; National Renewable Energy Laboratory (NREL),  
679 Golden, CO., 2014.
- 680 (31) Elliott, D. C.; Hart, T. R.; Schmidt, A. J.; Neuenschwander, G. G.; Rotness, L. J.; Olarte,  
681 M. V.; Zacher, A. H.; Albrecht, K. O.; Hallen, R. T.; Holladay, J. E. Process Development  
682 for Hydrothermal Liquefaction of Algae Feedstocks in a Continuous-Flow Reactor. *Algal*  
683 *Res.* **2013**, *2* (4), 445–454. <https://doi.org/10.1016/j.algal.2013.08.005>.
- 684 (32) Park, J. B. K.; Craggs, R. J.; Shilton, A. N. Wastewater Treatment High Rate Algal Ponds  
685 for Biofuel Production. *Bioresour. Technol.* **2011**, *102* (1), 35–42.  
686 <https://doi.org/10.1016/j.biortech.2010.06.158>.
- 687 (33) Chiu, S.-Y.; Kao, C.-Y.; Chen, T.-Y.; Chang, Y.-B.; Kuo, C.-M.; Lin, C.-S. Cultivation of  
688 Microalgal *Chlorella* for Biomass and Lipid Production Using Wastewater as Nutrient  
689 Resource. *Bioresour. Technol.* **2015**, *184* (Supplement C), 179–189.  
690 <https://doi.org/10.1016/j.biortech.2014.11.080>.
- 691 (34) Pittman, J. K.; Dean, A. P.; Osundeko, O. The Potential of Sustainable Algal Biofuel  
692 Production Using Wastewater Resources. *Bioresour. Technol.* **2011**, *102* (1), 17–25.  
693 <https://doi.org/10.1016/j.biortech.2010.06.035>.
- 694 (35) Chen, W.-T.; Zhang, Y.; Zhang, J.; Yu, G.; Schideman, L. C.; Zhang, P.; Minarick, M.  
695 Hydrothermal Liquefaction of Mixed-Culture Algal Biomass from Wastewater Treatment  
696 System into Bio-Crude Oil. *Bioresour. Technol.* **2014**, *152*, 130–139.  
697 <https://doi.org/10.1016/j.biortech.2013.10.111>.
- 698 (36) Mehrabadi, A.; Craggs, R.; Farid, M. M. Wastewater Treatment High Rate Algal Pond  
699 Biomass for Bio-Crude Oil Production. *Bioresour. Technol.* **2017**, *224*, 255–264.  
700 <https://doi.org/10.1016/j.biortech.2016.10.082>.
- 701 (37) Hietala, D. C.; Faeth, J. L.; Savage, P. E. A Quantitative Kinetic Model for the Fast and  
702 Isothermal Hydrothermal Liquefaction of *Nannochloropsis* Sp. *Bioresour. Technol.* **2016**,  
703 *214*, 102–111. <https://doi.org/10.1016/j.biortech.2016.04.067>.
- 704 (38) Chen, W.-T.; Qian, W.; Zhang, Y.; Mazur, Z.; Kuo, C.-T.; Scheppe, K.; Schideman, L. C.;  
705 Sharma, B. K. Effect of Ash on Hydrothermal Liquefaction of High-Ash Content Algal  
706 Biomass. *Algal Res.* **2017**, *25*, 297–306. <https://doi.org/10.1016/j.algal.2017.05.010>.
- 707 (39) Valdez, P. J.; Tocco, V. J.; Savage, P. E. A General Kinetic Model for the Hydrothermal  
708 Liquefaction of Microalgae. *Bioresour. Technol.* **2014**, *163*, 123–127.  
709 <https://doi.org/10.1016/j.biortech.2014.04.013>.
- 710 (40) Posmanik, R.; Labatut, R. A.; Kim, A. H.; Usack, J. G.; Tester, J. W.; Angenent, L. T.  
711 Coupling Hydrothermal Liquefaction and Anaerobic Digestion for Energy Valorization

- 712 from Model Biomass Feedstocks. *Bioresour. Technol.* **2017**, *233* (Supplement C), 134–143.  
713 <https://doi.org/10.1016/j.biortech.2017.02.095>.
- 714 (41) Shen, R.; Liu, Z.; He, Y.; Zhang, Y.; Lu, J.; Zhu, Z.; Si, B.; Zhang, C.; Xing, X.-H. Microbial  
715 Electrolysis Cell to Treat Hydrothermal Liquefied Wastewater from Cornstalk and Recover  
716 Hydrogen: Degradation of Organic Compounds and Characterization of Microbial  
717 Community. *Int. J. Hydrog. Energy* **2016**, *41* (7), 4132–4142.  
718 <https://doi.org/10.1016/j.ijhydene.2016.01.032>.
- 719 (42) Vardon, D. R.; Sharma, B. K.; Blazina, G. V.; Rajagopalan, K.; Strathmann, T. J.  
720 Thermochemical Conversion of Raw and Defatted Algal Biomass via Hydrothermal  
721 Liquefaction and Slow Pyrolysis. *Bioresour. Technol.* **2012**, *109*, 178–187.  
722 <https://doi.org/10.1016/j.biortech.2012.01.008>.
- 723 (43) Edmundson, S.; Huesemann, M.; Kruk, R.; Lemmon, T.; Billing, J.; Schmidt, A.; Anderson,  
724 D. Phosphorus and Nitrogen Recycle Following Algal Bio-Crude Production via  
725 Continuous Hydrothermal Liquefaction. *Algal Res.* **2017**, *26*, 415–421.  
726 <https://doi.org/10.1016/j.algal.2017.07.016>.
- 727 (44) Canter, C. E.; Blowers, P.; Handler, R. M.; Shonnard, D. R. Implications of Widespread  
728 Algal Biofuels Production on Macronutrient Fertilizer Supplies: Nutrient Demand and  
729 Evaluation of Potential Alternate Nutrient Sources. *Appl. Energy* **2015**, *143*, 71–80.  
730 <https://doi.org/10.1016/j.apenergy.2014.12.065>.
- 731 (45) Peccia, J.; Haznedaroglu, B.; Gutierrez, J.; Zimmerman, J. B. Nitrogen Supply Is an  
732 Important Driver of Sustainable Microalgae Biofuel Production. *Trends Biotechnol.* **2013**,  
733 *31* (3), 134–138. <https://doi.org/10.1016/j.tibtech.2013.01.010>.
- 734 (46) Carey, D. E.; Yang, Y.; McNamara, P. J.; Mayer, B. K. Recovery of Agricultural Nutrients  
735 from Biorefineries. *Bioresour. Technol.* **2016**, *215*, 186–198.  
736 <https://doi.org/10.1016/j.biortech.2016.02.093>.
- 737 (47) Mu, D.; Min, M.; Krohn, B.; Mullins, K. A.; Ruan, R.; Hill, J. Life Cycle Environmental  
738 Impacts of Wastewater-Based Algal Biofuels. *Environ. Sci. Technol.* **2014**, *48* (19), 11696–  
739 11704. <https://doi.org/10.1021/es5027689>.
- 740 (48) Yu, G.; Zhang, Y.; Schideman, L.; Funk, T.; Wang, Z. Distributions of Carbon and Nitrogen  
741 in the Products from Hydrothermal Liquefaction of Low-Lipid Microalgae. *Energy Environ.*  
742 *Sci.* **2011**, *4* (11), 4587–4595. <https://doi.org/10.1039/C1EE01541A>.
- 743 (49) Ekpo, U.; Ross, A. B.; Camargo-Valero, M. A.; Williams, P. T. A Comparison of Product  
744 Yields and Inorganic Content in Process Streams Following Thermal Hydrolysis and  
745 Hydrothermal Processing of Microalgae, Manure and Digestate. *Bioresour. Technol.* **2016**,  
746 *200* (Supplement C), 951–960. <https://doi.org/10.1016/j.biortech.2015.11.018>.
- 747 (50) Biller, P.; Ross, A. B.; Skill, S. C.; Lea-Langton, A.; Balasundaram, B.; Hall, C.; Riley, R.;  
748 Llewellyn, C. A. Nutrient Recycling of Aqueous Phase for Microalgae Cultivation from the  
749 Hydrothermal Liquefaction Process. *Algal Res.* **2012**, *1* (1), 70–76.  
750 <https://doi.org/10.1016/j.algal.2012.02.002>.
- 751 (51) Darwish, M.; Aris, A.; Puteh, M. H.; Abideen, M. Z.; Othman, M. N. Ammonium-Nitrogen  
752 Recovery from Wastewater by Struvite Crystallization Technology. *Sep. Purif. Rev.* **2016**,  
753 *45* (4), 261–274. <https://doi.org/10.1080/15422119.2015.1119699>.
- 754 (52) Angelé, B.; Kirchner, K. The Poisoning of Noble Metal Catalysts by Phosphorus  
755 Compounds—I Chemical Processes, Mechanisms and Changes in the Catalyst. *Chem. Eng.*  
756 *Sci.* **1980**, *35* (10), 2089–2091. [https://doi.org/10.1016/0009-2509\(80\)85031-7](https://doi.org/10.1016/0009-2509(80)85031-7).

- 757 (53) Bartholomew, C. H. Mechanisms of Catalyst Deactivation. *Appl. Catal. Gen.* **2001**, *212* (1),  
758 17–60. [https://doi.org/10.1016/S0926-860X\(00\)00843-7](https://doi.org/10.1016/S0926-860X(00)00843-7).
- 759 (54) Vardon, D. R.; Moser, B. R.; Zheng, W.; Witkin, K.; Evangelista, R. L.; Strathmann, T. J.;  
760 Rajagopalan, K.; Sharma, B. K. Complete Utilization of Spent Coffee Grounds To Produce  
761 Biodiesel, Bio-Oil, and Biochar. *ACS Sustain. Chem. Eng.* **2013**, *1* (10), 1286–1294.  
762 <https://doi.org/10.1021/sc400145w>.
- 763 (55) Wang, T.; Camps-Arbestain, M.; Hedley, M.; Bishop, P. Predicting Phosphorus  
764 Bioavailability from High-Ash Biochars. *Plant Soil* **2012**, *357* (1–2), 173–187.  
765 <https://doi.org/10.1007/s11104-012-1131-9>.
- 766 (56) Jiang, Y.; Jones, S. B.; Zhu, Y.; Snowden-Swan, L.; Schmidt, A. J.; Billing, J. M.; Anderson,  
767 D. Techno-Economic Uncertainty Quantification of Algal-Derived Biocrude via  
768 Hydrothermal Liquefaction. *Algal Res.* **2019**, *39*, 101450.  
769 <https://doi.org/10.1016/j.algal.2019.101450>.
- 770 (57) Beal, C. M.; Gerber, L. N.; Sills, D. L.; Huntley, M. E.; Machesky, S. C.; Walsh, M. J.;  
771 Tester, J. W.; Archibald, I.; Granados, J.; Greene, C. H. Algal Biofuel Production for Fuels  
772 and Feed in a 100-Ha Facility: A Comprehensive Techno-Economic Analysis and Life  
773 Cycle Assessment. *Algal Res.* **2015**, *10*, 266–279.  
774 <https://doi.org/10.1016/j.algal.2015.04.017>.
- 775 (58) Barlow, J.; Sims, R. C.; Quinn, J. C. Techno-Economic and Life-Cycle Assessment of an  
776 Attached Growth Algal Biorefinery. *Bioresour. Technol.* **2016**, *220*, 360–368.  
777 <https://doi.org/10.1016/j.biortech.2016.08.091>.
- 778 (59) Sasongko, N. A.; Noguchi, R.; Ito, J.; Demura, M.; Ichikawa, S.; Nakajima, M.; Watanabe,  
779 M. M. Engineering Study of a Pilot Scale Process Plant for Microalgae-Oil Production  
780 Utilizing Municipal Wastewater and Flue Gases: Fukushima Pilot Plant. *Energies* **2018**, *11*  
781 (7), 1693. <https://doi.org/10.3390/en11071693>.
- 782 (60) Chen, W.-T.; Zhang, Y.; Lee, T. H.; Wu, Z.; Si, B.; Lee, C.-F. F.; Lin, A.; Sharma, B. K.  
783 Renewable Diesel Blendstocks Produced by Hydrothermal Liquefaction of Wet Biowaste.  
784 *Nat. Sustain.* **2018**, *1* (11), 702. <https://doi.org/10.1038/s41893-018-0172-3>.
- 785 (61) Helmer Pedersen, T.; Conti, F. Improving the Circular Economy via Hydrothermal  
786 Processing of High-Density Waste Plastics. *Waste Manag.* **2017**, *68*, 24–31.  
787 <https://doi.org/10.1016/j.wasman.2017.06.002>.
- 788 (62) Short, W.; Packey, D. J.; Holt, T. *A Manual for the Economic Evaluation of Energy*  
789 *Efficiency and Renewable Energy Technologies*; NREL/TP-462-5173; National Renewable  
790 Energy Lab., Golden, CO (United States), 1995. <https://doi.org/10.2172/35391>.
- 791

## Table of Contents Entry



Treatment efficacy and economic performance of an algal wastewater treatment and valorization system were evaluated at different seasons.